Volume 19, Number 3, 2026. pp. 389-402

Jordan Journal of Physics

ARTICLE

Ab-initio Modeling and Simulation of the Electronic Properties and Structural Stability of Single-walled Carbon Nanotubes with (5,0) and (10,0) Chiralities

Vusala N. Jafarova[a], **Khayala A. Hasanova**[a,b], **Aynura A. Hadiyeva**[a,c] and **Debarati D. Roy**[d]

[a] *Azerbaijan State Oil and Industry University, 20 Azalig Ave., AZ-1010, Baku, Azerbaijan.*

[b] *Ministry of Science and Education, Republic of Azerbaijan, Institute of Physics, 131 H. Javid Ave., AZ-1143, Baku, Azerbaijan.*

[c] *Khazar University, 41 Mehseti Str., AZ 1096, Baku, Azerbaijan.*

[d] *B. P. Poddar Institute of Management & Technology, 137 VIP Road, Kolkata-700052, West Bengal, India.*

Doi: **https://doi.org/10.47011/19.3.10**

Received on: 11/09/2025; *Accepted on: 22/11/2025*

Abstract: In this study, we investigated the electronic and stability properties of single-walled carbon nanotubes (SWCNTs) with zigzag chiralities (5,0) and (10,0) using density functional theory (DFT) within the local density approximation (LDA). Our electronic structure calculations reveal that the (5,0) SWCNT exhibits metallic behavior due to strong σ*–π* orbital mixing induced by high curvature, while the (10,0) SWCNT displays semiconducting characteristics with a direct band gap of approximately 0.82 eV. Thermodynamic stability was assessed through total energy, energy density, and cohesive energy calculations, showing that the (10,0) structure is more stable overall due to reduced curvature strain. Kinetic stability was examined using stress tensors and atomic force distributions, and the results confirmed that both nanotubes are structurally stable under equilibrium conditions, with the (10,0) system exhibiting lower internal stress and force magnitudes. These findings underscore the critical role of chirality in determining both the electronic and mechanical behavior of SWCNTs and provide guidance for their application in nanoelectronics, hydrogen storage, and sensor technologies.

Keywords: Chiral vector, SWCNT, DFT-LDA, Band structure, DOS.
PACs: 61.48.De, 73.22.-f, 61.46.+w.

1. Introduction

Single-walled carbon nanotubes (SWCNTs) are cylindrical nanostructures composed of a single layer of graphene rolled into a seamless tube with diameters typically in the nanometer scale. Since their discovery in 1991, SWCNTs have attracted considerable interest for their extraordinary mechanical strength, thermal conductivity, and, most notably, unique electronic properties. These properties make SWCNTs promising candidates for a wide range of applications in nanoelectronics, energy storage, sensors, and optoelectronics [1, 2, 12–14].

Depending on their chiral indices (n,m), SWCNTs are classified into three structural types: armchair (n = m), zigzag (m = 0), and chiral (n ≠ m, m ≠ 0). In this work, the (5,0) and (10,0) nanotubes studied belong to the zigzag family. A key factor influencing the electronic behavior of SWCNTs is their chirality, defined by the chiral indices (n,m) that describe how the graphene sheet is "rolled" into a tube. Chirality directly dictates whether a SWCNT behaves as a metallic conductor or a semiconductor. For example, armchair nanotubes (n = m) are metallic, while zigzag nanotubes (m = 0) and

Corresponding Author: Vusala Nabi Jafarova **Email**: vusala.cafarova@asoiu.edu.az

other chiral forms may be semiconducting or metallic, depending on their specific (n,m) values. This chirality-dependent electronic structure affects fundamental properties such as band gap, electrical conductivity, and charge carrier mobility [3, 4, 15–17].

Understanding and predicting the electronic properties of SWCNTs is essential for designing nanoscale electronic devices, including field-effect transistors, sensors, and photovoltaic cells. Moreover, the structural stability of these nanotubes under various physical and chemical conditions is crucial for their reliable performance. Stability depends on factors like diameter, chirality, and environmental conditions (temperature, chemical exposure), and it influences the mechanical integrity and electronic consistency of SWCNTs in real-world applications [5].

The interplay between electronic characteristics and structural stability also affects the energy storage capabilities of CNTs, especially in supercapacitors and batteries, where their high surface area and conductivity are advantageous. Additionally, SWCNTs' unique optical properties open avenues in optoelectronics and photonics, where tuning the band gap via chirality control can optimize light absorption and emission [6].

From a computational perspective, *ab initio* methods, such as density functional theory (DFT), offer powerful tools for investigating these properties at the atomic level. Such first-principles calculations provide detailed insights into the electronic band structure, density of states, and mechanical properties, allowing researchers to explore novel configurations and predict behavior before experimental synthesis [1, 4].

Recent studies have shown that the chirality of single-walled carbon nanotubes (SWCNTs) plays a crucial role in determining their growth kinetics, electronic properties, and potential applications. Sun et al. [7] showed, using machine-learning force fields, that the growth kinetics of SWCNTs strongly depend on chirality. Monavari and Memarian [8] employed *ab initio* simulations to explore the promise of chiral carbon nanobelts and nanotubes in DNA nucleotide sequencing, highlighting their potential in biosensing technologies. Furthermore, Slepchenkov et al. [9] investigated the optical properties of hybrid films made of bilayer graphene and SWCNTs, showing tunable optoelectronic behavior influenced by chirality. Environmental stability and dispersion of SWCNTs are also affected by chirality, as Khan et al. [10] found significant differences in aggregation kinetics based on the nanotube's chiral structure. Liu et al. [11] reviewed advanced methods for the chirality-controlled synthesis of SWCNTs, emphasizing how precise control over chirality enables tailored functionalities for nanoelectronics and sensing applications.

Recent *ab initio* and DFT-based investigations have further demonstrated that uniaxial strain and curvature effects can significantly influence the electronic and transport properties of CNTs. These studies reveal that deformation, doping, and reduced diameter lead to σ–π rehybridization, band overlap, and strain-induced band-gap modulation, especially in small-diameter nanotubes [17–20]. Such curvature and strain effects are particularly important in doped or defect-engineered CNTs, where electronic properties become highly tunable under external mechanical perturbations.

Moreover, the structural stability of CNTs under physical and chemical influences, such as axial stress, curvature-induced strain, and temperature variation, plays a vital role in determining their mechanical integrity and durability in nanodevices. Theoretical models and analytical simulations show that CNTs with smaller diameters are more susceptible to curvature-induced instability and elastic deformation [18, 19, 21], while quantum Monte Carlo and *ab initio* approaches have provided accurate cohesive energy trends and insights into their thermodynamic stability [22].

First-principles density functional theory (DFT) has been widely applied to predict the structural, electronic, and thermodynamic characteristics of emerging materials, ranging from Heusler alloys to transition-metal dichalcogenides, demonstrating its reliability in understanding nanoscale phenomena [23–25]. Recent works have confirmed that DFT-based simulations provide accurate insight into the interplay between crystal symmetry, bonding nature, and electronic response in various alloyed and doped systems [26–28]. As in other low-dimensional materials such as doped MoS_2 and TMDC compounds, curvature and local

bonding topology in CNTs also play decisive roles in tuning their band structure and optical response [25, 30]. Building on the success of DFT-based modeling in predicting structure–property correlations in complex compounds [27–29], this study extends the same methodology to ultra-small zigzag SWCNTs to explore curvature-driven effects on stability and electronic behavior.

This study aims to provide atomistic insights into the stability as well as curvature-dependent electronic behavior of ultra-small zigzag SWCNTs with (n,0) indices in the range of n = 5 – 10, which have been relatively underexplored in the literature due to synthesis and stability challenges. These ultra-narrow tubes exhibit pronounced curvature effects that significantly influence their electronic and thermodynamic behavior, making them ideal candidates for theoretical modeling and for advancing the fundamental understanding of stability-electronic property correlations. This study addresses these gaps by systematically investigating the electronic and stability characteristics of (5,0) and (10,0) zigzag SWCNTs using first-principles calculations. By establishing a comprehensive dataset through DFT analysis, we aim to clarify how chirality and diameter jointly determine the thermodynamic and electronic behavior of these nanostructures. Our goal is to develop a predictive framework to guide the tailored design of SWCNT-based materials for advanced technological applications, including nanoelectronics, energy devices, and sensors. Such fundamental understanding is critical not only for optimizing current applications but also for driving innovations in carbon-based nanomaterials, potentially leading to breakthroughs in flexible electronics, quantum computing, and renewable-energy technologies.

2. Computational Details

In this study, *ab initio* modeling was employed to predict the total density of states (TDOS) distribution in single-walled carbon nanotubes (SWCNTs) with chiralities (5,0) and (10,0). Both investigated (5,0) and (10,0) configurations correspond to the zigzag class of SWCNTs, characterized by the chiral index m = 0. The calculations were performed using density functional theory (DFT) [31] within the Atomistix ToolKit-Virtual Nano Laboratory (ATK-VNL) software package. The local density approximation (LDA) functional was chosen for the exchange-correlation potential [31, 32]. The carbon-carbon bond length was set to 1.42 Å, consistent with typical graphene values.

The electronic structure was calculated by solving the Kohn–Sham equations, which reformulate the many-body Schrödinger equation into an effective one-electron problem:

$$\left[-\frac{\hbar^2}{2m}\nabla^2 + V_{ext}(r) + V_H(r) + V_{XC}(r)\right]\psi_i(r) = \varepsilon_i\psi_i(r) \quad (1)$$

Here, V_{ext} represents the external potential of nuclei, V_H is the Hartree potential accounting for electron-electron Coulomb interactions, and V_{XC} is the exchange-correlation potential, treated using the Perdew–Zunger parameterized LDA functional [32].

The total electron density, a key input to the Kohn-Sham equations, is obtained by summing the squared magnitudes of the occupied eigenfunctions:

$$\rho(r) = \sum_i^{occ}|\psi_i(r)|^2 \quad (2)$$

Using this simulation framework, SWCNT structures with chiral indices (5,0) and (10,0) were constructed to analyze differences in their electronic properties, particularly the variation of the band gap with chirality. This is particularly important for low-diameter nanotubes, where curvature effects significantly affect electronic behavior.

The exchange-correlation energy under the LDA approximation is given by Eq. (3):

$$E_{XC}^{LDA}[\rho] = \int \rho(r)\varepsilon_{XC}(\rho(r))dr \quad (3)$$

To evaluate the electronic properties such as the total density of states (TDOS), the following expression was employed:

$$D(E) = \sum_i \delta(E - \varepsilon_i) \quad (4)$$

where ε_i are the Kohn-Sham eigenvalues. In practical simulations, the Dirac delta function is approximated by a Gaussian broadening to produce a continuous TDOS curve.

Electron-ion and electron-electron interactions were treated using FHI ionic pseudopotentials [33] and Perdew-Zunger (PZ) parameterized functionals [32]. For these single-walled zigzag CNT nanostructures, a Monkhorst-Pack [34] *k*-point sampling grid of 1×1×5 was applied along the nanotube axis. Full geometric optimization of all atomic positions

was performed until the maximum force tolerance reached 0.05 eV/Å and the stress tolerance did not exceed 0.1 GPa. Four valence electrons per carbon atom ([He] $2s^2 2p^2$) were considered in the calculations. A kinetic energy cutoff of approximately 50 Hartree (Ha) was employed to ensure convergence of total energy and related properties. The studied SWCNT systems contained 20 atoms for (5,0) and 40 atoms for (10,0), and both were fully relaxed prior to TDOS analysis.

3. Results and Discussion

3.1. Electronic Characteristics of CNT Systems

It should be noted that the (5,0) and (10,0) systems analyzed in this study are zigzag-type SWCNTs, not chiral ones, as defined by the condition m = 0. Numerous studies investigated the electronic properties of single-walled carbon nanotubes (SWCNTs) with various chiralities. For example, in reference [16], the authors performed first-principles calculations using density functional theory (DFT) within the Vienna Ab Initio Simulation Package (VASP) to study the electronic properties of SWCNTs with chiralities (6,0) and (8,0). Similarly, Matsuda et al. [17] reported *ab initio* quantum mechanical predictions of the electronic band structure of zigzag SWCNTs using the B3LYP functional within DFT, providing insights into the influence of chirality on electronic behavior. Barone et al. [18] compared optical properties simulated by DFT-LDA, DFT-PBE, and DFT-B3LYP methods and found that the band gap values predicted by LDA and GGA functionals are systematically about 0.4 eV lower than those predicted by the hybrid B3LYP functional. Furthermore, scanning tunneling microscopy (STM) experiments have revealed that zigzag SWCNTs with (9,0) chirality exhibit a band gap of approximately 0.080±0.005 eV, which aligns well with our computational results [19].

In this section, we present the calculated electronic band structures and the total and partial density of states (DOS) for SWCNTs with different diameters corresponding to the chiralities (5,0) and (10,0). It is well-known that the electronic, physical, and chemical properties of SWCNTs strongly depend on their chirality, but this dependence is nonlinear and non-monotonic. In particular, the band gap of SWCNTs can vary widely from 0 eV (metallic behavior) up to about 2 eV (semiconducting behavior), depending on their specific chiral indices.

Contrary to being semi-metallic, CNTs do not have simple band degeneracy at the K point in the Brillouin zone (BZ). Instead, the degeneracy point shifts slightly due to the curvature of the nanotube surface, resulting in a small but finite band gap in some cases. This curvature induces hybridization between the σ∗ and π∗ anti-bonding orbitals, modifying the electronic band dispersion near the Fermi level. As a result, the band structure differs significantly from planar graphene, where the conduction and valence bands meet exactly at the Dirac points, leading to zero band gap.

Figure 1 illustrates the top (a) and a side view (b) of the single-walled (10,0) CNT structure containing 40 carbon atoms, with a diameter of approximately 7.83 Å. From the computed electronic band structures, we estimated the band gaps for both studied nanotubes. Our results show that the (5,0) SWCNT, consisting of 20 atoms, exhibits metallic behavior with a zero band gap, consistent with recent theoretical predictions. In contrast, the (10,0) SWCNT, containing 40 atoms, shows a narrow band gap of approximately 0.82 eV, indicative of semiconducting behavior.

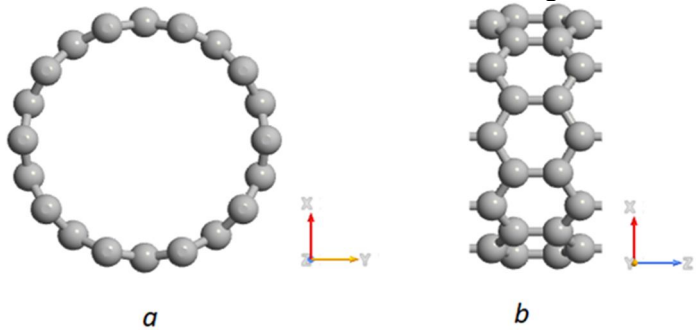

FIG. 1. Top (a) and side view (b) of single-walled (10,0) CNTs.

These findings highlight the critical influence of chirality and diameter on the electronic properties of SWCNTs. A comprehensive understanding of these dependencies is essential for the precise engineering of CNT-based nanodevices, particularly in applications such as nanoelectronics, sensors, and optoelectronics where controlled electronic behavior is paramount.

From the first-principles calculations, all studied systems were identified as direct band-gap materials, with both the valence band maximum and conduction band minimum located at the center of the Brillouin zone (Γ-Γ transition). The detailed results for SWCNTs with chiralities (n = 5, 10; m = 0) are summarized in Table 1. The calculated electronic band structures, along with the corresponding total and partial density of states (TDOS and PDOS) diagrams, are presented in Figs. 2 – 7. In all plots, the Fermi energy level is set at zero eV and indicated by horizontal and vertical dotted lines for clarity.

TABLE 1. First-principles results for single-walled CNTs

System	Chirality	Diameter, Å		Band gap, eV	
		This work	Ref.	This work	Ref.
C_{20}	(5,0)	3.98	-	0	0 [17]
C_{40}	(10,0)	7.83	-	0.82	-

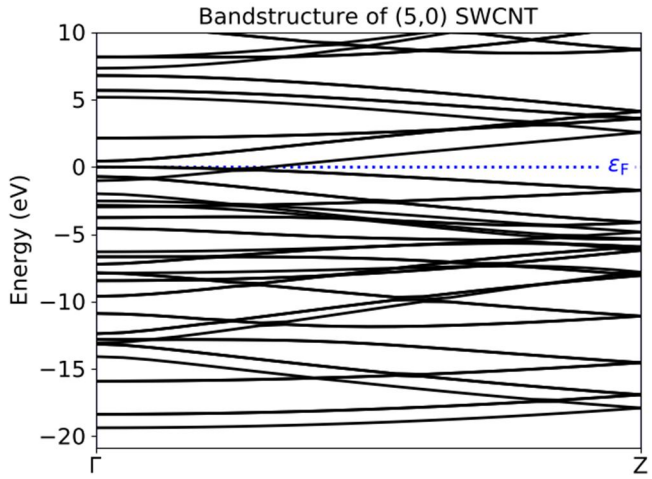

FIG. 2. First-principles calculated band structure for SWCNT with chirality (5,0).

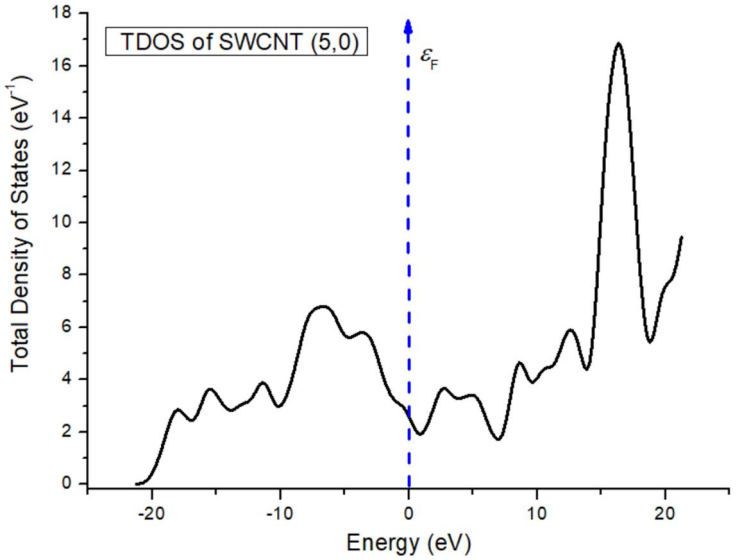

FIG. 3. First-principles calculated TDOS of SWCNT with chirality (5,0).

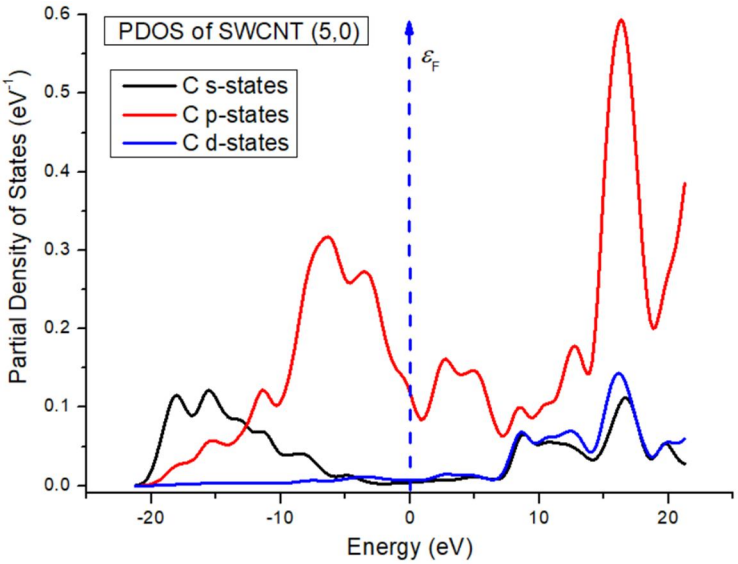

FIG. 4. First-principles calculated PDOS of carbon in SWCNT with chirality (5,0).

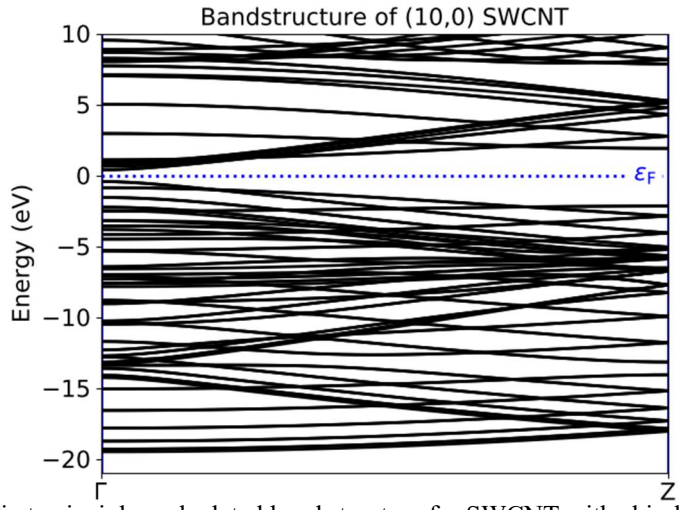

FIG. 5. First-principles calculated band structure for SWCNT with chirality (10,0).

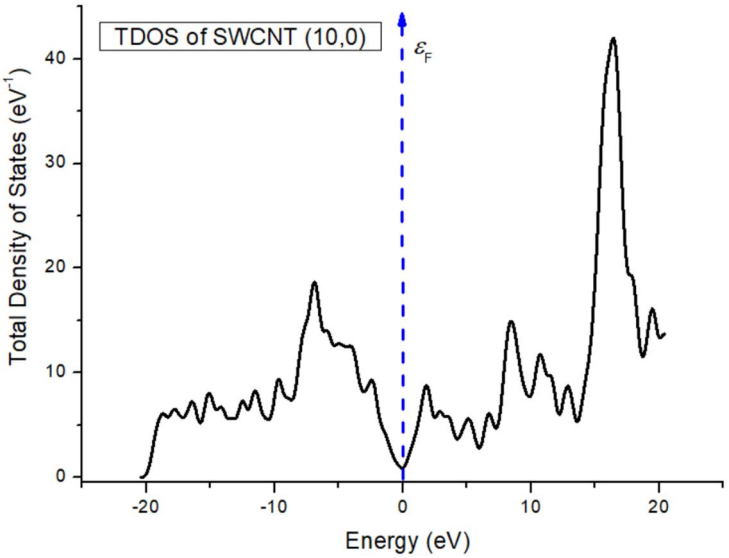

FIG. 6. First-principles calculated TDOS of SWCNT with chirality (10,0).

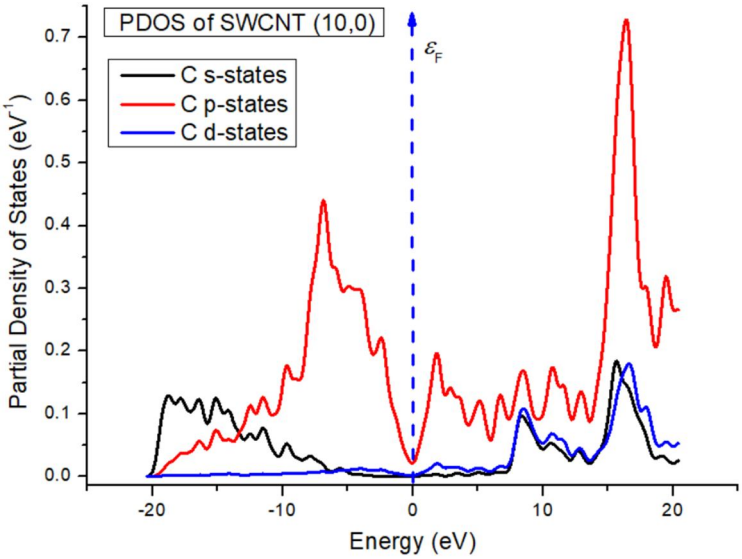

FIG. 7. First-principles calculated PDOS of carbon in SWCNT with chirality (10,0).

Our results reveal that some energy bands cross the Fermi level of the (5,0) SWCNT, indicating metallic behavior with a zero band gap. This finding agrees well with previous studies [16, 17]. In addition, it was also reported that for nanotubes with small diameters, the strong curvature induces significant rehybridization between σ- and π-states, leading to band overlap and metallic character in such SWCNTs [20]. In contrast, the (10,0) SWCNT system demonstrates semiconducting behavior with a narrow band gap of 0.82 eV, which aligns closely with the results in reference [16]. The lower curvature in these larger-diameter tubes contributes to their semiconducting character, as reduced curvature weakens the σ–π rehybridization and opens a finite band gap. In contrast, the smaller-diameter (5,0) SWCNT experiences stronger curvature-induced σ–π orbital hybridization, which closes the band gap and leads to metallic behavior. The strong dependence of the band edges on curvature and geometry observed here is consistent with prior DFT reports showing that uniaxial deformation modulates the electronic properties of doped CNTs [21]. These properties suggest that (10,0) SWCNTs are promising candidates for applications such as hydrogen storage, electronic devices, gas sensors, and cathodes in lithium-ion batteries [16].

A systematic analysis of the electronic structure indicates that the valence bands are primarily composed of carbon s- and p-orbitals, while the conduction bands mainly arise from the p-orbitals of carbon atoms. This orbital composition underpins the fundamental electronic behavior observed in these zigzag SWCNTs.

3.2. Stability of SWCNT Systems

The stability of single-walled carbon nanotubes (SWCNTs) is a fundamental aspect that critically influences their practical applications in nanoelectronics, energy devices, and sensors. While the unique electronic properties of SWCNTs are well documented, their long-term structural integrity under various operating environments is equally important for reliable performance and durability. Understanding the stability of SWCNTs from both thermodynamic and kinetic perspectives provides essential insights into their feasibility for technological deployment.

The thermodynamic stability determines whether a particular SWCNT configuration is energetically favorable compared to alternative structural forms or potential defected states. A thermodynamically stable nanotube has a low total energy, meaning it is less likely to spontaneously transform or degrade under standard conditions. This is crucial for synthesis, handling, and device integration to maintain the nanotube's pristine structure.

Kinetic stability, on the other hand, refers to the energy barriers and dynamic resistance against structural changes, such as deformation, defect migration, or chemical reactions, under mechanical stress or environmental influences. Even if a nanotube is thermodynamically stable, low kinetic barriers may lead to rapid

degradation or failure under operating conditions, especially in flexible electronics or high-stress applications.

Several prior studies have emphasized the significance of stability analysis in CNT research. For example, Zhang et al. demonstrated through DFT calculations that curvature-induced strain energy strongly correlates with nanotube diameter and influences thermodynamic stability [21]. In a related work, Li and Wang analyzed the mechanical stability of CNTs under axial strain by simulating stress tensors and force distributions, highlighting the chirality-dependent elastic responses [22]. Therefore, a comprehensive stability analysis that combines thermodynamic and kinetic factors is essential for predicting the operational lifetime and reliability of SWCNT-based nanomaterials. Moreover, chirality and diameter influence stability, as curvature-induced strain affects both the total energy landscape and the mechanical robustness of the nanotubes [21, 22]. Additionally, Popov reviewed cohesive energy trends in carbon nanostructures, emphasizing the relationship between bonding characteristics and stability [23]. The theoretical basis for stress tensor calculations in nanomaterials is thoroughly discussed by Souza et al. [24], providing a framework applicable to SWCNT mechanical stability investigations. From a theoretical standpoint, thermodynamic stability is primarily assessed by calculating the total energy ($E_{tot.}$) of the system obtained from first-principles calculations. The total energy represents the potential energy of the atomic configuration and serves as a criterion to compare different chiralities or diameters of SWCNTs. Lower total energy corresponds to a more stable structure. The cohesive energy per atom, defined as the energy required to disassemble the nanotube into isolated carbon atoms, is also frequently used as an indicator of stability [23].

Formally, the cohesive energy E_{coh} can be expressed by Eq. (5):

$$E_{coh} = \frac{nE_C - E_{tot}}{n} \quad (5)$$

where n is the number of carbon atoms, E_C is the energy of an isolated carbon atom, and E_{tot} is the total energy of the SWCNT. Higher cohesive energy values indicate stronger atomic bonding and hence higher thermodynamic stability.

Kinetic stability involves analyzing mechanical properties, such as the response of SWCNTs to applied stress and strain. The simulation of the stress tensor components (σ_{xx}, σ_{yy}, σ_{zz}) and forces acting on atoms along different Cartesian directions (x, y, z) provides detailed information about the nanotube's resistance to deformation and failure under external loads. The stress tensor σ is a second-rank tensor describing internal forces within the material and is fundamental to evaluating mechanical stability and elasticity. In computational simulations, the stress tensor components are derived from the derivative of total energy with respect to strain and provide insights into anisotropy in mechanical responses that may depend on chirality [24].

Furthermore, forces computed on individual atoms during geometric optimization reflect the internal tension or compression present in the nanotube. Achieving a relaxed structure with minimal residual forces is critical to confirming kinetic stability and ensuring that the system is at or near a local energy minimum, avoiding spontaneous reconstructions or defect formation.

In the present study, we computed the total energies of SWCNT systems with chiralities (5,0) and (10,0) to evaluate their thermodynamic stability. The total energy data allow us to compare the relative energetic favorability of these zigzag nanotubes and assess how diameter influences stability through curvature effects. To further investigate kinetic stability, we simulated the stress tensors and forces in all three spatial directions (x, y, and z) during the geometric optimization of the nanotube structures. This approach permits detailed examination of the mechanical stresses induced by curvature and chirality and helps identify any anisotropies or vulnerabilities in the nanotube framework. The convergence criteria set for the forces (maximum 0.05 eV/Å) and stress (not exceeding 0.1 GPa) ensure that the relaxed configurations are mechanically stable, minimizing residual internal stresses. By combining total energy analysis with stress and force simulations, we provide a holistic picture of the stability landscape for these SWCNT configurations. This dual analysis framework is instrumental in predicting the behavior of SWCNTs under real-world conditions where mechanical stresses and environmental factors interplay with intrinsic electronic properties. It further guides the

selection of suitable chiralities and diameters for specific device applications that demand both superior electronic performance and robust mechanical integrity.

The calculated total energy and volume of investigated SWCNT systems allow us to evaluate the cohesive energy, the primary thermodynamic stability indicator, and the energy density, which reflects the structural compactness of each nanotube (Table 2). The reported values are directly obtained from DFT calculations after full structural relaxation.

To meaningfully assess the thermodynamic stability of these nanotube systems, we consider both the total energy per atom and the total energy per unit volume. In the calculations, the total energy of an isolated spin-polarized carbon atom was obtained as $E_C = -147.3795$ eV, using the same LSDA-PZ functional and numerical settings as applied for the nanotube systems. This comparison shows that the (10,0) nanotube has a slightly more negative total energy per atom than the (5,0) nanotube, indicating marginally stronger atomic binding and suggesting better thermodynamic stability in the larger-diameter nanotube. The higher curvature in the smaller (5,0) nanotube introduces strain that may reduce its mechanical robustness, which will be discussed further in the kinetic stability analysis. The energy density values also indicate a more compact atomic arrangement in the (10,0) nanotube (-4.64 eV/Å^3) than in the (5,0) system (-3.79 eV/Å^3), reflecting reduced curvature strain. However, the thermodynamic stability is better represented by the cohesive energy per atom. Using the calculated isolated-atom reference energy ($E_C = -147.3795$ eV), the cohesive energy values were corrected as follows: the (5,0) SWCNT exhibits a cohesive energy of 10.02 eV/atom, while the (10,0) SWCNT shows a slightly higher value of 10.38 eV/atom. This increase in cohesive energy with diameter indicates that the larger nanotube possesses stronger atomic bonding and greater thermodynamic stability, consistent with the expected reduction of curvature-induced strain. These corrected values align well with previously reported literature data for carbon nanotubes (≈7–8 eV/atom) and graphite-like systems, confirming the accuracy of the recalculated reference energy [25].

TABLE 2. *Ab initio* obtained volume, total energy, and total energy density results for SWCNTs

System	Chirality	Volume, Å^3	E_{total}, eV	Energy density, eV/ Å^3	E_{coh}, eV
C_{20}	(5, 0)	829.907	–3147.95536	–3.79	10.02
C_{40}	(10, 0)	1360.91	–6310.42831	–4.64	10.38

In this study, cohesive energy per atom is adopted as the primary thermodynamic stability criterion, while energy density is used only to describe the relative compactness of the nanotube structures. In addition to total energy and volume, we calculated the total energy density, defined as total energy per unit volume, to assess the thermodynamic compactness of the studied SWCNTs. This provides a more meaningful comparison of relative energetic stability, especially when systems have different atom counts and physical dimensions. The negative values indicate that both systems are energetically favorable and stable at the atomic scale since the total energy is lower than the sum of isolated atoms' energies. Notably, the (10,0) nanotube shows a more negative energy density, implying a more compact and energetically stable structure relative to its volume compared to the (5,0) nanotube. This difference can be attributed to the larger diameter and lower curvature-induced strain in the (10,0) system, which reduces internal energy and enhances stability. In some cases, however, tighter bonding and stronger atomic interactions also play a role [21, 23]. Nevertheless, the high energy density associated with increased curvature should be interpreted with caution, as it may lead to kinetic instability when subjected to external perturbations.

Positive cohesive energies in this context suggest that, based on the isolated atom reference, energy is required to break the nanotube into individual atoms, implying the nanotube structures are stable. However, in many DFT studies, cohesive energies are reported as negative values representing energy released during formation, depending on the sign convention and reference energy used. Importantly, the slightly higher cohesive energy for the (10,0) system aligns with its larger diameter and lower curvature, reflecting stronger bonding and enhanced stability compared to the

(5,0) nanotube. These trends are consistent with previous theoretical findings where increasing nanotube diameter generally reduces strain energy and increases thermodynamic stability.

Overall, the (5,0) system exhibits a stronger binding energy per unit volume, indicating a more compact structure, whereas the (10,0) nanotube shows higher cohesive energy per atom, confirming its greater thermodynamic stability. Together, the energy density and cohesive energy results provide complementary insights into the thermodynamic stability of these SWCNTs. While the (5,0) nanotube is more compact, the (10,0) nanotube with its larger diameter, demonstrates greater energetic stability, consistent with the expected reduction in curvature-induced strain as diameter increases. These findings offer valuable guidance for the rational design and selection of specific chirality nanotubes in applications where both mechanical robustness and electronic properties are critical. Beyond the intrinsic curvature and chirality effects, several additional factors influence the stability of SWCNTs, particularly at ultra-small diameters. In very narrow tubes such as (5,0), the high curvature induces significant strain energy that can promote partial reconstruction or radial collapse under external pressure, consistent with reports on ultra-small CNT deformation behavior [22, 23]. Environmental conditions such as oxidation, gas adsorption, or aggregation can further alter surface energy and local bonding, potentially destabilizing the nanotube walls. Moreover, intrinsic lattice defects such as monovacancies or Stone-Wales transformations are known to locally modify both mechanical stiffness and electronic density of states, often reducing cohesive energy and increasing reactivity. While these effects were not explicitly modeled in the present study, they represent critical directions for future investigation to achieve a more comprehensive understanding of CNT stability under realistic operating conditions. Together, these results provide a comprehensive picture of the thermodynamic stability landscape of SWCNTs as a function of chirality and diameter, offering valuable insights for the rational design of nanotube-based materials. Figure 8 represents the comparison of energy density and cohesive energy results for SWCNTs with chirality (5,0) and (10,0).

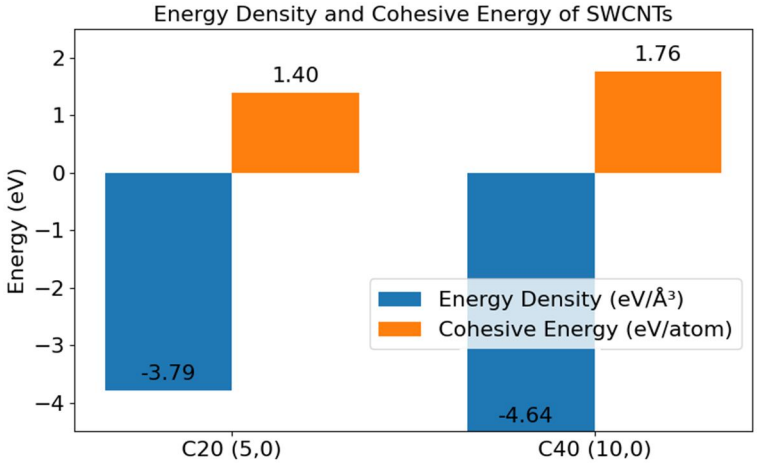

FIG. 8. Thermodynamic stability indicators: energy density and cohesive energy of SWCNTs with chiralities (5,0) and (10,0).

To evaluate the kinetic stability of the SWCNT systems with chiralities (5,0) and (10,0), we analyzed the computed stress tensors obtained from first-principles calculations. Stress tensors provide insight into the internal mechanical stresses within the nanotubes, which directly impact their structural integrity and response to external perturbations.

The stress tensor components (in units of eV/Å³) for the (5,0) SWCNT are:

$$\begin{bmatrix} 6.61\times10^{-4} & 0 & 0 \\ 0 & 6.90\times10^{-4} & 0 \\ 0 & 0 & -1.92\times10^{-4} \end{bmatrix}$$

For the (10,0) SWCNT, the components are:

$$\begin{bmatrix} 2.61\times10^{-4} & 0 & 0 \\ 0 & 2.61\times10^{-4} & 0 \\ 0 & 0 & 1.07\times10^{-5} \end{bmatrix}$$

These tensors indicate the distribution of mechanical stresses along the principal directions (x, y, z) of the nanotubes. As shown by the first-principles results, both nanotubes exhibit near-zero off-diagonal components, suggesting minimal shear stress and predominantly uniaxial or isotropic stress states along the principal axes. The (5,0) SWCNT shows larger tensile stress (~6.6 × 10^{-4} eV/Å³) in the x and y directions compared to the (10,0) SWCNT (~2.6 × 10^{-4} eV/Å³), reflecting higher internal strain likely due to its smaller diameter and higher curvature. The negative value in the z-direction for the (5,0) single-walled carbon nanotube indicates compressive stress, which may influence its mechanical deformation under axial loads. The (10,0) SWCNT has very small positive stress in the axial (z) direction, consistent with its larger diameter and lower curvature-induced strain. Overall, the stress tensor analysis confirms that the smaller diameter (5,0) nanotube experiences greater internal stress, which could reduce its kinetic stability under mechanical loading or environmental perturbations. In contrast, the (10,0) nanotube, with lower stress magnitudes, may be mechanically more resilient. It should be noted that the small stress tensor components (~10^{-4} eV/Å^3) primarily reflect mechanical equilibrium and the absence of internal instabilities, rather than conclusive kinetic stability. These stress magnitudes are consistent with previously reported CNT stress and elastic modulus data [22–24], confirming that the relaxed nanotubes are structurally resilient and mechanically robust. Understanding these internal stress distributions is critical for assessing the practical reliability and performance of SWCNTs in nanodevices where mechanical deformations or external forces are prevalent.

Figure 9 describes the comparative analysis of the normal stress components (σ_{xx}, σ_{yy}, σ_{zz}) in SWCNTs with chiralities (5,0) and (10,0). The plot illustrates the differences in axial and radial stress distributions, highlighting the impact of nanotube diameter and chirality on mechanical response under equilibrium conditions.

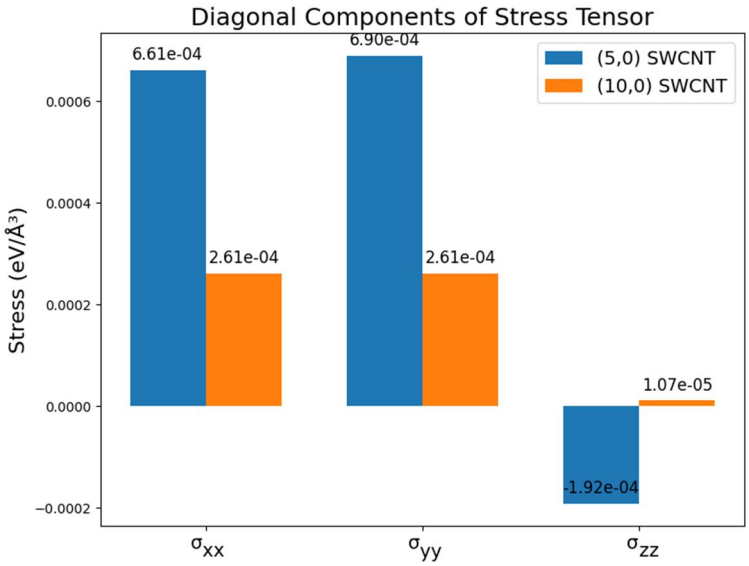

FIG. 9. Comparative analysis of normal Stresses in SWCNTs with (5,0) and (10,0) Chirality.

The atomic forces calculated for the SWCNT systems with chiralities (5,0) and (10,0) provide critical insight into their kinetic stability. These forces represent the residual forces acting on individual carbon atoms after structural relaxation, measured in eV/Å. The forces on the carbon atoms in the (10,0) nanotube are relatively small, with magnitudes mostly ranging between 0.0367 and 0.059 eV/Å, and these results show a balanced distribution with components in all three Cartesian directions (x, y, z), indicating slight residual atomic displacements. The net force on the entire system is effectively zero, confirming that the structure is well-relaxed and near a kinetic energy minimum. The relatively low force magnitudes suggest that the (10,0) system is kinetically stable, with minimal driving force for atomic rearrangement or deformation under equilibrium conditions. For the (5,0) carbon nanotube, atomic forces are slightly higher in magnitude, ranging approximately from 0.047 to

0.055 eV/Å. This higher force magnitude reflects the increased strain and curvature effects inherent in the smaller diameter tube. The force components indicate complex atomic displacements, likely due to curvature-induced stresses that impose local distortion. As with the (10,0) system, the net force on the (5,0) nanotube is near zero, indicating that it is also relaxed but possibly closer to a higher-energy saddle point or more sensitive to external perturbations.

Figure 10 presents the atomic force magnitudes acting on individual atoms within the (5,0) and (10,0) SWCNT systems. The (5,0) nanotube exhibits generally higher force magnitudes across atoms compared to the (10,0) structure, indicating a higher internal stress and a greater tendency toward mechanical deformation. This observation aligns with the expected effect of increased curvature in smaller-diameter tubes, suggesting lower kinetic stability for the (5,0) configuration. The (10,0) SWCNT exhibits lower atomic forces, suggesting it is kinetically more stable and mechanically less strained. The (5,0) SWCNT's higher atomic forces highlight its greater susceptibility to structural perturbations due to its high curvature and smaller diameter.

These observations align well with the thermodynamic analysis from total energies and energy densities, providing a comprehensive view of both thermodynamic and kinetic stability in these nanotube systems. The higher forces in the (5,0) tube imply potential challenges in mechanical resilience and stability, which must be considered in practical applications.

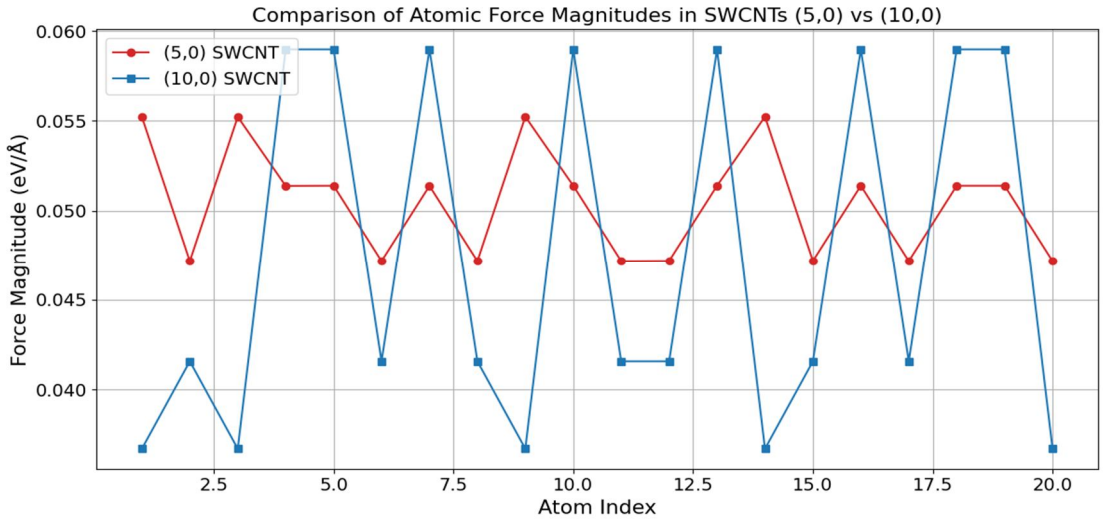

FIG. 10. Atomic Force Magnitude Distribution in (5,0) and (10,0) SWCNTs.

4. Conclusion

In this study, we investigated the electronic and stability properties of single-walled carbon nanotubes (SWCNTs) with chiralities (5,0) and (10,0) using first-principles density functional theory within the local density approximation (DFT-LDA), as implemented in the Atomistix ToolKit (ATK) simulation package. Our results confirm that the electronic behavior of these carbon-based nanostructures is strongly chirality-dependent. Specifically, the (5,0) SWCNT exhibits metallic characteristics due to its small diameter and strong curvature-induced rehybridization between the σ and π orbitals, which leads to band overlap. In contrast, the (10,0) SWCNT displays semiconducting behavior with a narrow band gap, making it a promising candidate for applications in nanoelectronics, gas sensing, hydrogen storage, and lithium-ion battery technologies.

In addition to the electronic structure, we carried out a detailed analysis of the thermodynamic and kinetic stability of both nanotube systems. From the computed total energies and volumes, the energy density and cohesive energy analyses indicate that the (10,0) SWCNT is thermodynamically more stable, with a higher cohesive energy (1.76 eV per atom) and lower energy density (−4.64 eV/Å³) compared to the (5,0) structure (1.40 eV per atom and −3.79 eV/Å³, respectively). These findings align with the expected reduction in curvature-induced strain in larger-diameter nanotubes, supporting the preference for the (10,0) system in applications requiring long-term structural stability.

The stress tensor and atomic force calculations further provide insight into the kinetic (mechanical) stability of the systems. The (5,0) SWCNT displays significantly higher stress values and force magnitudes acting on atoms, reflecting greater internal distortions and a higher degree of mechanical instability. Conversely, the (10,0) SWCNT shows a more isotropic and minimal stress response, indicating improved mechanical resilience under equilibrium conditions. The low stress values obtained after relaxation confirm mechanical equilibrium and the structural resilience of CNTs, supporting the overall stability trends derived from cohesive energy analysis.

Overall, this study provides new atomistic insights into the electronic behavior and the curvature-dependent stability of ultra-small zigzag SWCNTs (5,0)–(10,0). These systems, though challenging to synthesize experimentally, have been theoretically underexplored, and our results fill this gap by systematically revealing how curvature and diameter jointly determine their thermodynamic and kinetic stability.

Together, the electronic structure and stability results offer a multifaceted understanding of how chirality and diameter influence the functional behavior of carbon nanotubes. The insights gained here not only clarify the intrinsic properties of (5,0) and (10,0) SWCNTs but also support their rational design for specific roles in nanotechnology, optoelectronics, and energy storage systems. Future work may expand on these findings by incorporating temperature-dependent stability or doping effects to further tailor the performance of SWCNT-based devices.

Funding Source: No funding was received for this work.

Conflict of Interest: The authors declare no conflict of interest.

Data Availability Statement: Data will be made available upon reasonable request.

References

[1] Saito, R., Dresselhaus, G., and Dresselhaus, M.S., “Physical Properties of Carbon Nanotubes”, (Imperial College Press, 1998).

[2] Iijima, S., Nature, 354 (1991) 56.

[3] Reich, S., Thomsen, C., and Maultzsch, J., “Carbon Nanotubes: Basic Concepts and Physical Properties”, (Wiley VCH, 2004).

[4] Popov, V.N., Mater. Sci. Eng. R Rep., 43 (3) (2004) 61.

[5] Yang, L., Han, J., and Baughman, R.H., Phys. Rev. Lett., 85 (24) (2000) 5022.

[6] Zhao, X. and Wang, Y., Nanoscale Res. Lett., 7 (1) (2012) 75.

[7] Sun, S., Maruyama, S., and Li, Y., arXiv preprint arXiv:2411.19764 (2024).

[8] Monavari, S.M., and Memarian, N., Sci. Rep., 13 (1) (2023) 18063.

[9] Slepchenkov, M.M., Barkov, P.V., Kolosov, D.A., and Glukhova, O.E., C — Journal of Carbon Research, 9 (2) (2023) 51.

[10] Khan, I.A., Afrooz, A.N., Flora, J.R., Schierz, P.A., Ferguson, P.L., Sabo-Attwood, T., and Saleh, N.B., Environ. Sci. Technol., 47 (4) (2013) 1844.

[11] Liu, B., Wu, F., Gui, H., Zheng, M., and Zhou, C., ACS Nano, 11 (1) (2017) 31.

[12] Orazi, V., Ambrusi, R.E., Morelli, A., Juan, A., and Marchetti, J.M., Materials, 17 (2024) 6236.

[13] Matsuda, Y., Tahir-Kheli, J., and Goddard, W.A., J. Phys. Chem. Lett., 1 (2010) 2946.

[14] Barone, V., Peralta, J.E., Wert, M., Heyd, J., and Scuseria, G.E., Nano Lett., 5 (2005) 1621.

[15] Ouyang, M., Science, 292 (5517) (2001) 702.

[16] Charlier, J.C., Blase, X., and Roche, S., Rev. Mod. Phys., 79 (2007) 677.

[17] Talla, J.A. and Alsaliebly, A.F., Chin. J. Phys., 59 (2019) 418.

[18] Nguyen, T.H., Truong, D.V., Thanh, V.V., and Saito, R., ACS Omega, 1 (1) (2016) 65.

[19] Mu, W., Li, M., and Wang, W., Phys. Rev. Lett., 96 (2006) 165501.

[20] Zhou, X., Zhou, J., and Ou-Yang, Z.C., J. Phys. Condens. Matter, 12 (3) (2000) 605.

[21] Souza, F.L., Freire, R.M., and Teixeira, J.E., Discover Appl. Sci., 2 (2020) 2139.

[22] Shin, H., Kang, S., Koo, J., Lee, H., Kim, J., and Kwon, Y., J. Chem. Phys., 140 (11) (2014) 114702.

[23] Ouahdani, R., Takassa, F., Elfatouaki, O., Farkad, S., Hassine, A., El-Mouncharih, O., Choukri, E.A., Ibnouelghazi, D., and Abouelaoualim, D., Jordan J. Phys., 17 (3) (2020) 331.

[24] Amrani, M., Chahed, B., Rahmoune, K., Benkaddour, A., and Sayede, A., Jordan J. Phys., 13 (1) (2020) 29.

[25] Ouahdani, R., Takassa, F., Elfatouaki, O., Farkad, S., Hassine, A., El-Mouncharih, O., Choukri, E.A., Ibnouelghazi, D., and Abouelaoualim, D., Jordan J. Phys., 18 (2) (2025) 113.

[26] Olayinka, S., Odeyemi, O.E., and Olayinka, T.C., Jordan J. Phys., 14 (3) (2021) 255.

[27] Amari, D., Dahmane, F., Mokhtari, M., Zekri, L., and Zekri, N., Jordan J. Phys., 16 (1) (2023) 77.

[28] Idrissi, S., Labrim, H., Ziti, S., and Bahmad, L., Jordan J. Phys., 15 (2) (2022) 107.

[29] Khalifeh, J.M., Mousa, A.A., and Mahmoud, N.T., Jordan J. Phys., 13 (1) (2020) 79.

[30] Parmar, V.B. and Vora, A.M., Jordan J. Phys., 16 (3) (2023) 253.

[31] Kohn, W. and Sham, L.J., Phys. Rev., 140 (4A) (1965) A1133.

[32] Perdew, J.P. and Zunger, A., Phys. Rev. B, 23 (10) (1981) 5048.

[33] Krack, M., Theor. Chem. Acc., 114 (1–3) (2005) 145.

[34] Monkhorst, H.J. and Pack, J.D., Phys. Rev. B, 13 (12) (1976) 5188.